Pertanika J. Sci. & Technol. 26 (3): 979 - 990 (2018)

SCIENCE & TECHNOLOGY

Journal homepage: http://www.pertanika.upm.edu.my/

Preparation and Thermal Properties of Cellulose Acetate/ Polystyrene Blend Nanofibers via Electrospinning Technique

Rosdi, N. H., Mohd Kanafi, N. and Abdul Rahman, N.*

Department of Chemistry, Faculty of Science, Universiti Putra Malaysia, 43400 UPM, Serdang, Selangor, Malaysia

ABSTRACT

Cellulose acetate (CA) is an interesting material due to its wide spectrum of utilities across different domains ranging from absorbent to membrane filters. In this study, polystyrene (PS) nanofibres, and cellulose acetate/polystyrene (CA/PS) blend nanofibres with various ratios of CA: PS from 20: 80 to 80: 20 were fabricated by using electrospinning technique. The SEM images show that the nanofibres exhibited non-uniform and random orientation with the average fibre diameter in the range of 100 to 800 nm. It was found that the incorporation of PS had a great effect on the morphology of nanofibre. At high proportion of PS, no or less beaded CA/PS nanofibres were formed. Thermal properties of the composite nanofibres were investigated by using thermogravimetric analysis (TGA) and differential scanning calorimetry (DSC) techniques. The TGA results showed thermal stability of CA/PS nanofibres were higher than pristine CA.

Keywords: Cellulose acetate, electrospinning, nanofibres, polystyrene

INTRODUCTION

Cellulose is the most abundant renewable natural polymer material and resource. Most of the plant cells are made up of cellulose. Just like polysaccharides, cellulose is widely used in medical applications because it is non-toxic, has a high swelling ability and stable temperature and pH variations (Raucci et al., 2014). Cellulose acetate (CA) is part of cellulose derivatives and produced by reacting cellulose with acetic anhydride with the presence of sulfuric acid as a catalyst (Yan & Yu, 2012). Cellulose acetate is well known as a biodegradable and biocompatible polymer.

Recently, cellulose acetate based nanofibres have been gaining attention because its fabrication and disposal does not damage the environment (Konwarh, Karak, &

ARTICLE INFO

Article history:
Received: 09 May 2017
Accepted: 25 April 2018

E-mail addresses:
nurulhusnarosdi73@gmail.com (Rosdi, N. H.)
nafeesakanafi@yahoo.com (Mohd Kanafi, N.)
a_norizah@upm.edu.my (Abdul Rahman, N.)
*Corresponding Author

ISSN: 0128-7680

Misra, 2013b). Cellulose acetate nanofibre has high potential to be used in various applications like in bone regeneration (Yamaguchi et al., 2016), gas sensor (Qingqing et al., 2016), supercapacitor (Yang et al., 2015), filtration (Sehaqui et al., 2016) and drug delivery (Konwarh, Karak, & Misra, 2013a). Composites/blend polymers consists of synthetic and biodegradable polymers will provide novel properties to the materials. Researchers have prepared cellulose acetate blend with other synthetic polymer to form nanofibre (Zhijiang, Yi, Haizheng, Jia, & Liu, 2016; Gopiraman, Fujimori, Zeeshan, Kim, & Kim, 2013; Zhou, He, Cui, & Gao, 2011). According to Konwarh et al., (2013b) electrospun CA in the presence of other polymer such as poly(vinyl pyrrolidone) (PVP), poly(ethylene oxide) (PEO) and poly(butyl acrylate) (PBA) have improved tensile strength and increased its stability (Konwarh, 2013a). However, there has not been much focus on how to improve thermal properties of CA based nanofibres.

Polystyrene (PS) is a cheap and strong polymer that is widely used in the plastic industry. The PS nanofibre have been widely used as filter media, ion exchanger and separator (An, Shin, & Chase, 2006). Additionally, numerous studies have focused on PS as a composite material and the result showed an improvement in material performance compared to that without PS Kaya, Kaynak, & Hacaloglu, 2016; Jia, Chen, Yu, Zhang, & Dong, 2015; Zhang, Wen, Hu, Zhang, & Liu, 2010). The PS is also able to increase thermal stability of composites material due to an increase in the mobility of the macromolecule chains which results in a to more ideal crystalline pattern (Kaya et al., 2016; Meireles, Filho, Assunc, & Zeni, 2007). In addition, Mathew et al., and Kaya et al., showed PS enhanced the thermal stability of the composite PS with natural rubber (NR) (Mathew, Packirisamy, & Thomas, 2001) and nanocomposite with organoclay (Kaya et al., 2016) respectively.

In general, nanomaterials are defined as materials that are manufactured and used at a scale less than 100 nm. However, for polymer nanofibres, it has been widely accepted for fibre diameter less than 1000 nm (Lubasova, Niu, & Lin, 2015; Stone, Gosavi, Athauda, & Ozer, 2013; Zhou et al., 2011; An et al., 2006). Many techniques can be used to produce polymer nanofibres including electrospinning, self-assembly, template synthesis and phase separation (Huang, Zhang, Kotaki, & Ramakrishna, 2003). Among these techniques, electrospinning is considered simple, cost effective, and suitabile to produce very long fibres from various polymers and composite materials (Abdul Rahman et al., 2014), (Konwarh, 2013a). Polymer nanofibres produced high surface area to volume ratio that make the electrospun fibrous membranes suitable for use in many applications such as filtration, sensors, catalysis and protective clothing (Huang, Zhang, Kotaki, & Ramakrishna, 2003).

This study focused on producing PS nanofibres and CA/PS composite nanofibres by using electrospinning technique. PS was chosen in this study to improve thermal stability of the CA. The thermal properties of the composite were investigated using differential scanning calorimetry (DSC) and thermogravimetric analysis (TGA).

MATERIALS AND METHODS

Polystyrene and cellulose acetate (Mn = 30,000) was supplied by BDH Chemicals. Dimethylformamide (DMF) and tetrahydrofuran (THF) used as solvents were purchased from the Fischer Chemical. All chemicals were used as received without further purification.

Preparation of PS nanofibres

PS nanofibres were prepared using mixed solution of DMF and THF (1:1). PS solution was filled in a 5 mL syringe fitted with a steel needle and was placed on the syringe pump whereas the collector was 8.0 cm away from the tip of needle. By using 35 to 45 kV of voltage and 2 mL/h for flow rate, PS nanofibres were synthesised. The PS nanofibre was fabricated based on five different concentrations from 0.5 to 10 w/v%.

Preparation of cellulose acetate/ polystyrene (CA/PS) nanofibres

Electrospinnable solution of CA/PS nanofibre was prepared by dissolving appropriate amount of CA and PS in the mixed solution of DMF and THF (1:1) with total concentration of 2.5 w/v%. The CA/PS solution was filled in a 5mL syringe attached to a steel needle. An aluminum foil was placed 8.0 cm distance from the needle. The electrospinning process was carried out at room temperature in a horizontal spinning configuration, using the fixed applied voltage of 40 kV and pump rate of 2 ml/h. The humidity was kept at around 40%. The electrospun fibres were collected directly on an aluminum foil which was used to collect substrate.

Characterisations

The morphology of the electrospun nanofibres was observed using Jeol JSM-6400 scanning electron microscopy (SEM). The sample for SEM observations was put on the aluminium stubs and was coated with gold prior image the nanofibres morphology. The electrospun fibre diameter was measured using SEM images. The average of diameter for each sample was calculated from at least 30 measurements. For beaded fibres, only the areas of the fibres between beads were measured. Thermal properties of the composite nanofibres were determined using differential scanning calorimetry (DSC) (Model DSC Mettler Toledo 822°) from 50°C to 250°C with a heating rate of 10°C/min under nitrogen flow at 50 mL/min. Thermogravimetric analysis (TGA) (Mettler Toledo thermogravimetric model TGA/SDTA 851) measurement was done under nitrogen gas. The sample was heated from 35°C to 500°C with a heating rate of 10°C/min.

RESULTS AND DISCUSSION

Morphology of the Nanofibres

Electrospun PS nanofibres 2.5 w/v% and CA/PS composite nanofibres with various CA to PS ratios were prepared using electrospinning technique. The total concentration of CA/PS was kept constant at 2.5 w/v%, but the ratio of CA to PS was varied between 20% and 80%. Figure 1 shows the SEM images of electrospun PS and CA/PS nanofibre. PS nanofibres have average fibre diameter of 249 ± 70 nm.

As shown in Table 1, the average fibre diameter decreased from 229 ± 200 nm to 111 ± 50 nm as the ratio of PS in CA/PS nanofibre reduced from 80% to 20%. However, the formation of beads was increased as CA content in the composite nanofibres increased. The optimum morphology of CA: PS nanofibres was found at 40% of CA. However, in this study, CA alone cannot be electrospun by using electrospinning technique.

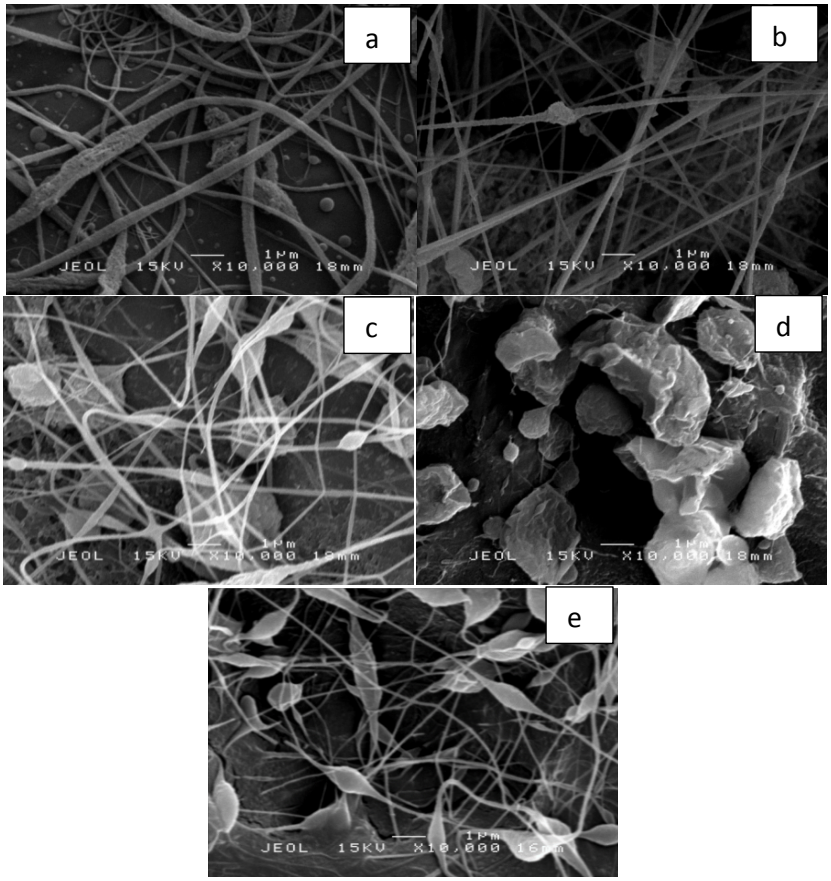

Figure 1. SEM images of CA/PS blend nanofibre with CA: PS ratios of (a) PS (b) 20:80 (c) 40:60 (d) 60:40 and (e) 80:20

Table 1
Fibre diameter of PS and CA/PS composite nanofibre

CA:PS	Average fibre diameter (nm) ± Standard Deviation
20:80	229 ± 200
40:60	186 ± 60
60:40	-
80:20	111 ± 50
PS	249 ± 70

Spectroscopic study of the nanofibres

Figure 2 shows IR spectra of PS nanofibre, pristine CA and CA/PS nanofibres with different ratios of CA and PS. The PS nanofibres have three main peaks in the spectrum corresponding to PS structure that consists of alkyl group and aromatic ring. The absorption bands of IR

spectrum of PS nanofibres at wavenumber 3000 to 3100 cm^{-1} belong to the aromatic C-H stretching vibration of CH_2 groups on the PS main chain. A peak at 1598 cm^{-1} shows the present of aromatic C=C skeletal and a peak at 1448 cm^{-1} which corresponds to aromatic C-H bending. Absorption peaks at around 1100 cm^{-1}, 765 cm^{-1} and 700 cm^{-1} corresponding to vibrations of C-H bending of the benzene ring, C–H out-of-plane bend, and CH_2 rocking mode respectively (Nair, Hsiao, & Kim, 2008). The IR spectrum of pristine CA consists of a broad absorption band at 3300-3500 cm^{-1}, which is belongs to stretching O-H group. The absorption bands at 2700- 2900 cm^{-1} are attributed to C-H stretching of alkane. A peak at 1035 cm^{-1} corresponds to C-O-C (ether linkage) from glycosidic units.

The IR spectrum of the composite CA/PS nanofibres shows combination peaks of CA and PS. The O-H peaks that belong to CA appear very small and become clearly visible when the ratio of CA was increased from 40% to 80%. The stretching O-H vibration peak slightly shifted to 3029 cm^{-1} from 3417 cm^{-1} and the intensity of the peak reduced as the concentration of CA is reduced. This is due to the hydrogen bonds formed between the OH groups in CA are reduced as CA content becomes less in the composite nanofibres. The C-H aromatics peak was clearly observed in the IR spectra in Figure 2(a) to (d). However, the peak disappeared in Figure 2(e) and (f). A peak in between 1704.42 cm^{-1} to 1741.42 cm^{-1} that belong to carbonyl group shifted to higher wavenumber indicates there is an interaction between CA and PS in CA/PS nanofibres (Chen, Wang, & Huang, 2011).

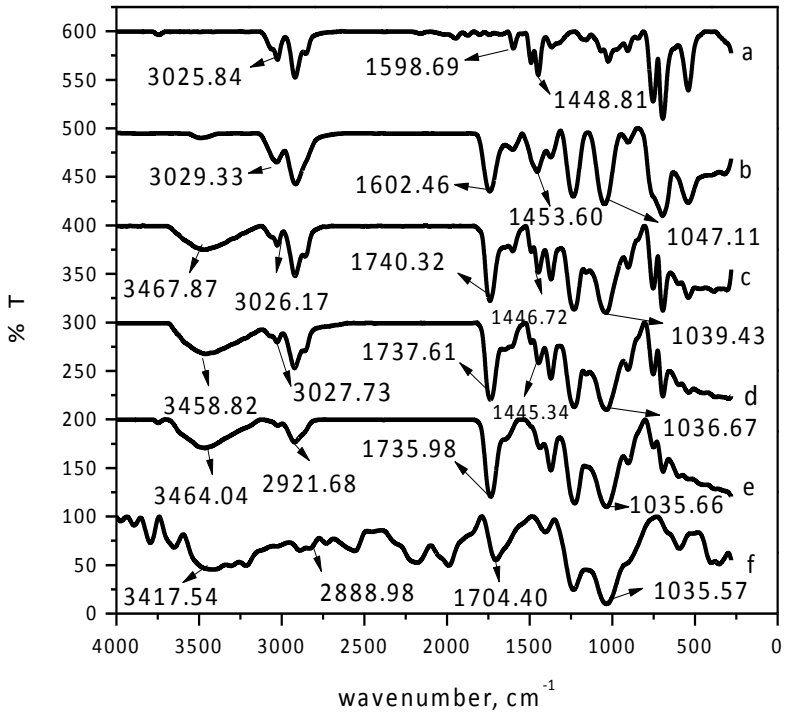

Figure 2. FTIR spectra of (a) PS nanofibre and CA/PS blend nanofibre; (b) 20/80; (c) 40/60; (d) 60/40; (e) 80/20; and (f) CA pristine

Thermogravimetric Analysis of the nanofibres

Figure 3 shows TGA thermograms of CA pristine and PS nanofibre. As can be seen from the TGA results and PS nanofibres show only a single degradation step. According to Uyar et al., (2008) polystyrene degrades in a single step starting at 250°C until 500°C under nitrogen atmosphere. The degradation range for PS nanofibres was between 210°C and 463°C is due to rupture of PS chains (Meireles, 2006). CA pristine undergoes two steps of degradation. The first peak of degradation started at 76°C and the second decomposition peak was at 342°C. 10% of weight loss was recorded at first peak and almost 80% weight loss was occurred at second peak. Similar result was obtained by Meireles et al., where CA underwent major degradation between 330°C and 450°C (Arthanareeswaran, Thanikaivelan, Srinivasn, Mohan, & Rajendran, 2004).

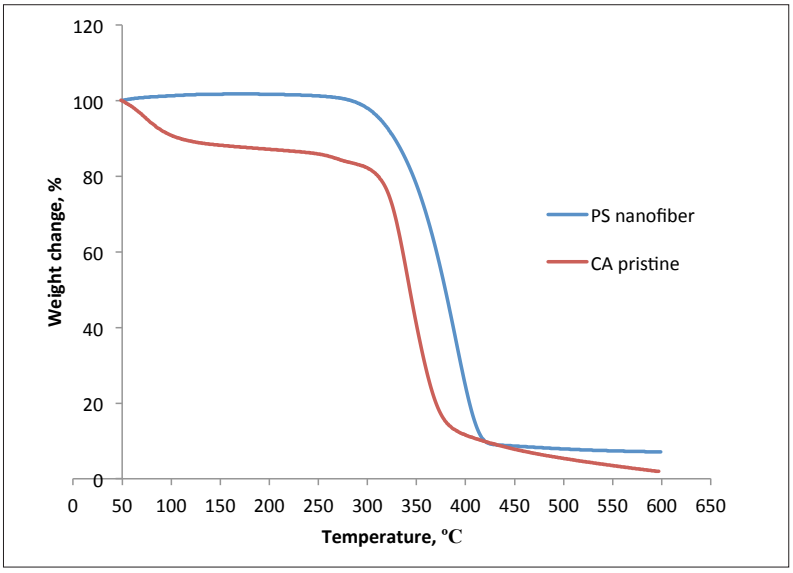

Figure 3. TGA thermograms of PS nanofibre and CA pristine

Figure 4 shows TGA thermograms of PS nanofibres, CA pristine and CA/PS nanofibres. DTG peaks of CA and the nanofibres are shown in Figure 5 and summarised in Table 2. The first step is the elimination of moisture, and the second, third and fourth steps are decomposition of cellulose acetate and polystyrene chains. The elimination of moisture was occurred at between 30°C to 120°C. The moisture mostly comes from CA due to present of hydroxyl group that can have hydrogen bond with water. The second and third degradation temperature of composite nanofibre was shifted to the higher temperature as the PS content in the composite nanofibre was increased (Table 2). This is due to PS having higher thermal stability than CA (Arthanareeswaran, 2004). Pure CA has lower thermal stability than PS nanofibre and CA/PS nanofibres. At high ratio PS, the blend nanofibres have higher thermal stability than CA/PS nanofibre with high ratio CA. This is probably due to the presence of PS that could increase the crystallinity of PS composite nanofibres (Ding et al., 2003).

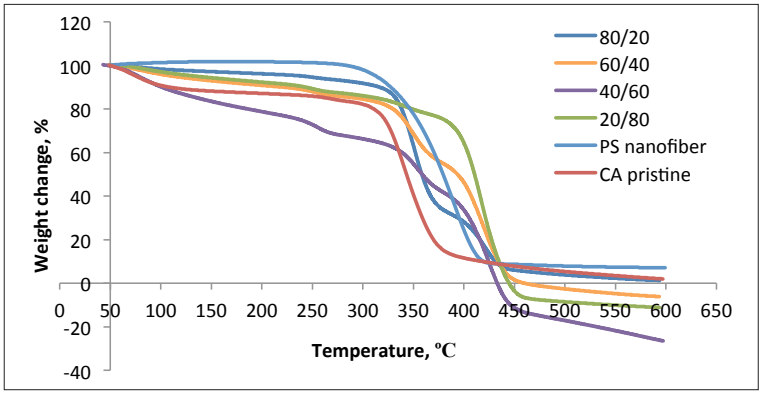

Figure 4. TGA thermograms of CA/PS blend nanofibre with CA: PS ratios of 80/20, 60/40, 40/60, 20/80, CA pristine and PS nanofibre

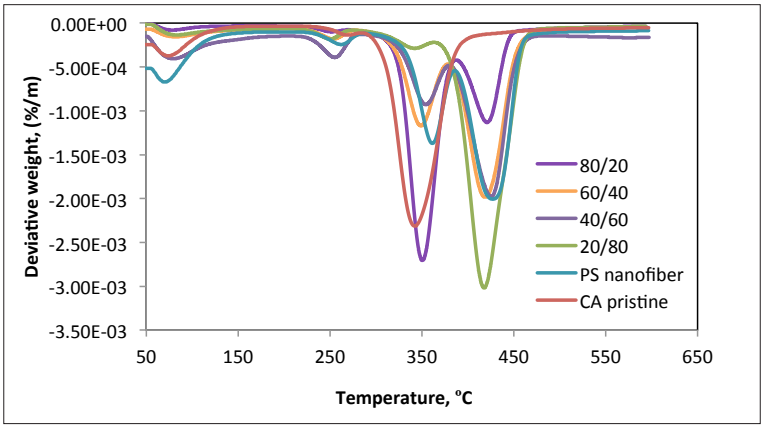

Figure 5. DTG thermograms of CA/PS blend nanofibres with CA: PS ratios of 20/80, 40/60, 60/40 and 80/20, CA pristine and PS nanofibres

Table 2
DTG results for CA/PS composite nanofibre, CA pristine and PS nanofibre

CA/PS composite nanofibres ratio	1st step (°C)	2nd step (°C)	3rd step (°C)	4th step (°C)
CA pristine	76	-	342	
PS nanofibre	-	-	390	
20/80	81	249	-	417
40/60	79	255	-	425
60/40	81	253	348	419
80/20	76	-	350	421

DSC Analysis of PS nanofibres

Figure 6 shows the first scan DSC thermogram of CA pristine, PS nanofibres and CA/PS nanofibres with different ratios of CA to PS. The DSC thermograms of CA/PS have similar pattern as previously reported for CA/PS blend film (Meireles et al., 2006). All the composite

nanofibres show an endothermic peak at temperature from 50°C to 100°C. The endothermic peak of CA is due to the outflow of water. This in agreement with observed TGA thermogram. The endothermic peak is shifted to lower temperature for CA/PS nanofibres compared to CA pristine. Incorporation of PS to CA could increase the hydrophobicity of the composite nanofibres and prevent water absorption.

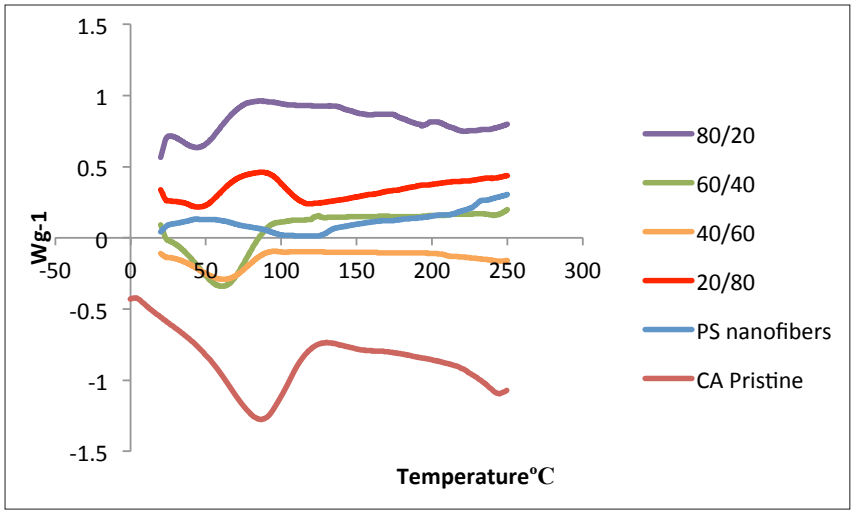

Figure 6. DSC thermograms of PS nanofibres and CA/PS blend nanofibres with CA: PS ratios of 20/80, 40/60, 60/40, 80/20and PS nanofibres

According to Holmes et al. (2010), glass transition (T_g) of PS occurs between 74°C – 109°C and the melting temperature is at 240°C to 250°C. However, in Figure 6, neither peaks of T_g nor the melting peak was observed for PS and CA/PS nanofibres in the thermograms. The absence of T_g peak was possibly because certain polymer only showed the T_g value after second run of DCS test (Meireles et al., 2006), (Hyon, Cha, & Ikada, 1987) or it overlapped with endothermic peak of CA at around 100°C.

According to Meireles et al., (2006), temperature of fusion increased sharply as the amount of PS added was increased indicating the increase in crystallinity (Zhijiang et al., 2016). This is due to the movement of the macromolecule chains caused by PS. This leads to a perfect crystalline pattern. However, the peak is not observed in the CA/PS nanofibres, possibly due to compact structure of the nanofibres preventing the movement of molecular chains to crystallise.

CONCLUSION

CA/PS composite nanofibres were successfully prepared using electrospinning technique. The SEM images showed the prepared composite nanofibre had smooth nanofibres morphology as the PS ratio in blend polymer solution increased. All electrospun nanofibre and composite nanofibre exhibited submicron sized fibre diameters, ranging from 100 to 800 nm. The thermal

degradation properties of CA/PS nanofibres were investigated using TGA and DSC techniques. CA/PS composites nanofibre has higher thermal stability than CA pristine. The DSC results showed mixing CA with PS reduced outflow of water. Unlike the CA/PS film, the absence of crystallisation peak in DSC thermograms of composite nanofibres indicated the nanofibres have low tendency to crystallise.

ACKNOWLEDGEMENTS

This work was supported by the Ministry of Education Malaysia under project code 01-02-14-1568FR and Putra Grant 9407050.

REFERENCES

An, H., Shin, C., & Chase, G. G. (2006). Ion exchanger using electrospun polystyrene nanofibers. *Journal of Membrane Science, 283*(1–2), 84–87. http://doi.org/10.1016/j.memsci.2006.06.014

Arthanareeswaran, G., Thanikaivelan, P., Srinivasn, K., Mohan, D., & Rajendran, M. (2004). Synthesis, characterization and thermal studies on cellulose acetate membranes with additive. *European Polymer Journal, 40*(9), 2153–2159. http://doi.org/10.1016/j.eurpolymj.2004.04.024

Chen, C., Wang, L., & Huang, Y. (2011). Electrospun phase change fibers based on polyethylene glycol/cellulose acetate blends. *Applied Energy, 88*(9), 3133–3139. http://doi.org/10.1016/j.apenergy.2011.02.026

Ding, R., Hu, Y., Gui, Z., Zong, R., Chen, Z., & Fan, W. (2003). Preparation and characterization of polystyrene/graphite oxide nanocomposite by emulsion polymerization. *Polymer Degradation and Stability, 81*(3), 473–476. http://doi.org/10.1016/S0141-3910(03)00132-0

Gopiraman, M., Fujimori, K., Zeeshan, K., Kim, B. S., & Kim, I. S. (2013). Structural and mechanical properties of cellulose acetate/graphene hybrid nanofibers: Spectroscopic investigations. *Express Polymer Letters, 7*(6), 554–563. http://doi.org/10.3144/expresspolymlett.2013.52

Huang, Z. M., Zhang, Y. Z., Kotaki, M., & Ramakrishna, S. (2003). A review on polymer nanofibers by electrospinning and their applications in nanocomposites. *Composites Science and Technology, 63*(15), 2223–2253. http://doi.org/10.1016/S0266-3538(03)00178-7

Hyon, S., Cha, W., & Ikada, Y. (1987). Polymer Bulletin 9. *Polymer Bulletin, 29*(3), 119–126. http://doi.org/10.1007/BF00310794

Jia, Y., Chen, L., Yu, H., Zhang, Y., & Dong, F. (2015). Graphene oxide/polystyrene composite nanofibers on quartz crystal microbalance electrode for the ammonia detection. *RSC Advances, 5*(51), 40620–40627. http://doi.org/10.1039/C5RA04890G

Kaya, H., Kaynak, C., & Hacaloglu, J. (2016). Thermal degradation of polystyrene composites. Part II. The effect of nanoclay. *Journal of Analytical and Applied Pyrolysis, 120*, 194–199. http://doi.org/10.1016/j.jaap.2016.05.005

Konwarh, R., Karak, N., & Misra, M. (2013a). Electrospun cellulose acetate nano fibers: The present status and gamut of biotechnological applications. *Biotechnology Advances, 31*(4), 421–437. http://doi.org/10.1016/j.biotechadv.2013.01.002

Konwarh, R., Misra, M., Mohanty, A. K., & Karak, N. (2013b). Diameter-tuning of electrospun cellulose acetate fibers: A Box-Behnken design (BBD) study. *Carbohydrate Polymers, 92*(2), 1100-1106. http://doi.org/10.1016/j.carbpol.2012.10.055

Lubasova, D., Niu, H., & Lin, T. (2015). RSC Advances Hydrogel properties of electrospun polyvinylpyrrolidone and polyvinylpyrrolidone. *RSC Advances, 5*, 54481–54487. http://doi.org/10.1039/C5RA07514A

Mathew, A. P., Packirisamy, S., & Thomas, S. (2001). Studies on the thermal stability of natural rubber/polystyrene interpenetrating polymer networks: Thermogravimetric analysis. *Polymer Degradation and Stability, 72*(3), 423–439. http://doi.org/10.1016/S0141-3910(01)00042-8

Meireles, C. D. S., Filho, G. R., de Assunção, R. M., Zeni, M., & Mello, K. (2007). Blend compatibility of waste materials—cellulose acetate (from sugarcane bagasse) with polystyrene (from plastic cups): diffusion of water, FTIR, DSC, TGA, and SEM study. *Journal of Applied Polymer Science, 104*(2), 909-914. http://doi.org/10.1002/app

Nair, S., Hsiao, E., & Kim, S. H. (2008). Fabrication of electrically-conducting nonwoven porous mats of polystyrene-polypyrrole core-shell nanofibers via electrospinning and vapor phase polymerization. *Journal of Materials Chemistry, 18*(42), 5155–5161. http://doi.org/Doi 10.1039/B807007e

Qingqing, Z., Fenglin, W., Qufu, H., Yang, Z., Chen, Y., Zhang, J., … & Aspects, E. (2016). A room temperature ammonia gas sensor based on cellulose / TiO_2 / PANI composite nanofibers. *Colloids and Surface A: Physicochemical and Engineering Aspects, 494*, 248–255. http://doi.org/10.1016/j.colsurfa.2016.01.024

Rahman, N. A., Srinivas, A. G., & Travas-Sejdic, J. (2014). Spontaneous stacking of electrospun conjugated polymer composite nanofibers producing highly porous fiber mats. *Synthetic Metals, 191*, 151–160. http://doi.org/http://dx.doi.org/10.1016/j.synthmet.2014.03.006

Sehaqui, H., Mautner, A., de Larraya, U. P., Pfenninger, N., Tingaut, P., & Zimmermann, T. (2016). Cationic cellulose nanofibers from waste pulp residues and their nitrate, fluoride, sulphate and phosphate adsorption properties. *Carbohydrate Polymers, 135*, 334–340. http://doi.org/10.1016/j.carbpol.2015.08.091

Yamaguchi, K., Prabakaran, M., Ke, M., Gang, X., Chung, I. M., Um, I. C., … & Kim, I. S. (2016). Highly dispersed nanoscale hydroxyapatite on cellulose nanofibers for bone regeneration. *Materials Letters, 168*, 56–61. http://doi.org/http://dx.doi.org/10.1016/j.matlet.2016.01.010

Yan, J., & Yu, D. G. (2012). Smoothening electrospinning and obtaining high-quality cellulose acetate nanofibers using a modified coaxial process. *Journal of Materials Science, 47*(20), 7138–7147. http://doi.org/10.1007/s10853-012-6653-2

Yang, C., Chen, C., Pan, Y., Li, S., Wang, F., Li, J., … & Li, D. (2015). Flexible highly specific capacitance aerogel electrodes based on cellulose nanofibers, carbon nanotubes and polyaniline. *Electrochimica Acta, 182*, 264–271. http://doi.org/10.1016/j.electacta.2015.09.096

Zhang, X., Wen, S., Hu, S., Zhang, L., & Liu, L. (2010). Electrospinning preparation and luminescence properties of Eu(TTA)3phen/polystyrene composite nanofibers. *Journal of Rare Earths, 28*(3), 333–339. http://doi.org/10.1016/S1002-0721(09)60108-3

Zhijiang, C., Yi, X., Haizheng, Y., Jia, J., & Liu, Y. (2016). Poly(hydroxybutyrate)/cellulose acetate blend nanofiber scaffolds: Preparation, characterization and cytocompatibility. *Materials Science and Engineering C, 58*, 757–767. http://doi.org/10.1016/j.msec.2015.09.048

Zhou, W., He, J., Cui, S., & Gao, W. (2011). Preparation of electrospun silk fibroin/Cellulose Acetate blend nanofibers and their applications to heavy metal ions adsorption. *Fibers and Polymers, 12*(4), 431–437. http://doi.org/10.1007/s12221-011-0431-7